3D Tracking of Small Moving Targets from a Multi-Target Tracking Algorithm Applied to Millimeter-wave Radar Images

Etienne Dedic, D. Henry, M. Lihoreau, Hervé Aubert

3D Tracking of Small Moving Targets from a Multi-Target Tracking Algorithm Applied to Millimeter-wave Radar Images

E. Dedic[#$1], D. Henry[^2], M. Lihoreau[$*3], H. Aubert[#$4]

[#]LAAS, CNRS, 31400 Toulouse, France
[^]Ovalie-Innovation, 32000 Auch, France
[$]Toulouse University, Toulouse, France
[*]CRCA-CBI, CNRS, Université Toulouse III, 31000 Toulouse, France
{[1]ededic, [2]dhenry, [4]haubert}@laas.fr, [3]mathieu.lihoreau@univ-tlse3.fr

***Abstract* — In this paper, we report a technique for tracking multiple small moving targets using a millimeter-wave Frequency-Modulated Continuous-Wave radar. Radar images are obtained from raw radar data collected by a radar system that performs a digital beamscanning in the azimuth plane and a mechanical beamscanning in the elevation plane. Trajectories of several targets in the scene are estimated from a new multi-target tracking (MT^2) algorithm based on the calculation of the global nearest neighbors. We demonstrate the effectiveness of this algorithm from the tracking of two moving targets. Our preliminary experimental results obtained for short range (up to 2.0 meters) outdoor detection of small tags pave the way for future research on tracking tagged flying insects and could therefore be useful for studying the behavior and ecology of pollinators.**

***Keywords* — multi-target tracking, millimeter-wave, radar imaging, remote sensing.**

I. INTRODUCTION

How small flying insects such as bees, wasps and flies move across space to forage is a fundamental question in biology, with applications for pollination and pest control [1]. Detailed tracking of insect movements in their natural environment is challenging, even at short ranges. For instance, tracking a flying bee requires to monitor a small target (<2cm long) with high velocity (up to 20km/h) moving in the three-dimensional (3D) space. Optical tracking systems have been proposed (see, e.g., [2]-[4]), but require multiple sensors to resolve the insects position in 3D and are sensitive to brightness. To fill this technological gap, we recently proposed a millimeter-wave (mm-wave) Frequency-Modulated Continuous-Wave (FM-CW) radar tracking system [5]. This radar imaging system allowed to track 3D flights of a single bumblebee in a limited volume during 5.2 minutes. Building on these previous encouraging results, we now aim to track simultaneously multiple insects moving in the scanned scene.

Multi-Object Tracking (MOT) algorithms have been proposed to resolve the tracks of multiple targets from a set of detections (see overviews of MOT in [6] and [7]). One of the main applications of this class of algorithms is real-time video surveillance (e.g., for traffic surveillance). In the present article, we introduce a new algorithm for tracking multiple small moving targets using a mm-wave FM-CW radar. We call it the *Multi-Target Tracking* (MT^2) algorithm. It is based on the Global Nearest Neighbours approach, which is one of the simplest MOT methods (see, e.g., [7]). The MT^2 algorithm estimates the tracks of multiple targets from a set of unclassified radar detections. The detections are assigned to one or multiple tracks from the computation of a specific cost function. We first demonstrate the performances of the MT^2 algorithm by estimating tracks on simulated data. Then, we apply the MT^2 algorithm to experimental radar data obtained from two small moving targets as preliminary work for the tracking of multiple flying insects.

The article is organized as follows: in Section II, we introduce the used radar-based detection system, and in Section III we present the MT^2 algorithm. Next, in Section IV we report and discuss the very first experimental demonstration of the proposed MT^2 algorithm to track small tags moving around an artificial flower.

II. MM-WAVE RADAR DETECTION SYSTEM

A. Radar scanning system

To collect mm-wave radar data from the scene of interest, we use the *RBK2* FM-CW MIMO radar with an operating frequency of 77GHz commercialized by *INRAS GmbH*. This sensor steers the radar beam electronically in azimuth using 16 channels. We add the beam scanning in elevation by using a rotating reflector (20cm-by-25cm rectangular metallic plate) placed at a distance of d_r=15cm from the front-end of the radar (see Figure 1). This reflector is set to rotate by a DC motor at a speed of 500rpm, while the FM-CW measurement rate is 1ms. The scene is then scanned in average 16.7 times per second. The power transmitted by the radar is of 10mW (see [5] for more technical information about this radar scanning system).

B. Acquisition of radar images

To obtained 3D radar images from the collected raw radar data, we apply a 2D-MUSIC algorithm [8], which estimates a so-called *range-azimuth pseudo-spectrum* on each elevation plane collected for each FM-CW radar measurement. The set of range-azimuth pseudo-spectra on successive elevation planes allows to map the radar echo level in 3D from the scanned scene.

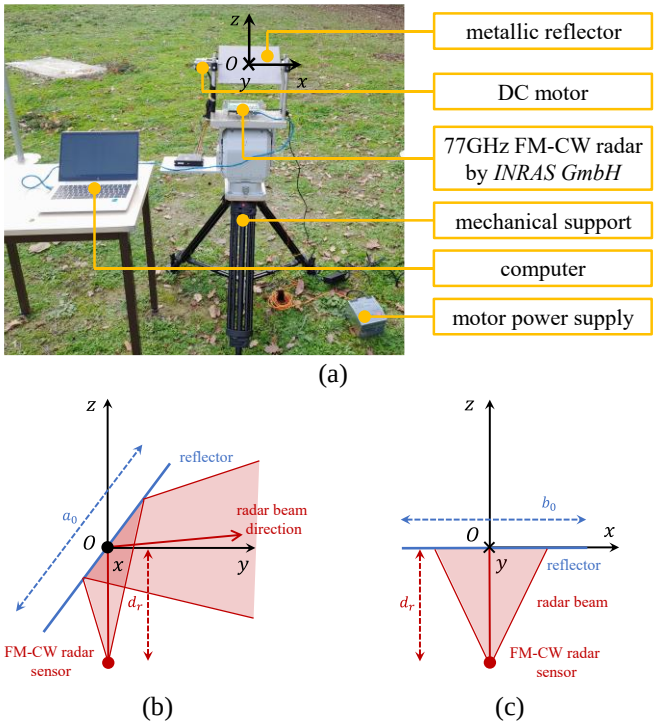

Fig. 1. (a) Annotated photo of the mm-wave FM-CW radar system used to track small moving targets in the 3D space. The Cartesian (x, y and z) coordinate system and the origin set on the rotating axis centered with the radar front-end are shown. Schematic representation of the beam scanning system projected on (b) Oyz plane and (c) Oxz plane (a_0=20cm and b_0=25cm are respectively the width and length of the rectangular plate used as a reflector).

C. Detection algorithm

To detect the targets in the radar images derived from the collected radar data, we apply the detection algorithm reported in [9] and based on the isoline segmentation technique developed in [10]. We use the DBSCAN clustering to group close detections in a so-called *cluster* from which the centroid is considered as a new detection instead of those from the cluster. Electromagnetic clutter generated by static objects in the scene is mitigated thanks to an algorithm [9] that relies on a calibration radar measurement of the scene without any targets present. So-called *clutter calibration* detections are then derived from the calibration radar images and are used to classify as "clutter" or "target" the unclassified detections derived from the radar images of the scene in presence of the target.

III. MT^2 ALGORITHM

A. Description of the MT^2 algorithm

Let D be the set of N_D detections computed by applying the detection algorithm on radar images. Each detection of the set D is characterized by its position in the Cartesian coordinate system (O, x, y, z) and its associated timestamp t_i with $i \in [1,N_D]$. The original process from which tracks are reconstructed by the proposed MT^2 algorithm follows the steps summarized in Figure 2. The detection set D is first sorted monotonically by time, that is, either by increasing time or by decreasing time (respectively *forward* and *backward* reconstruction methods). Tracks are then reconstructed sequentially from the sorted detection set using the Global Nearest Neighbours (GNN) approach. The tracks reconstruction is facilitated by splitting the set D into M subsets D_m so-called *gates* with m an integer ranging from 1 to M. The number of detections inside each gate is determined both by a constant time interval δt_s and a maximum number n_{max} of detections per gate. This step is called *gating*. Each detection from gate D_m can be a part of existing tracks or can be the first detection of a new track. To evaluate all possible tracks, the permutations of detections in the gate D_m are considered. A permutation is denoted P_q where q is an integer ranging from 1 to $Q = n_m!$ with n_m the number of detections in gate D_m. This step is called *permutation*. Next, for each permutation P_q, the detections are added to the previously defined tracks. To estimate the most probable association of a given detection to a track, we define the cost function C as follows :

$$C(\delta p, \delta \alpha, \delta t) = w_p \frac{\delta p}{\delta p_0} + w_\alpha \frac{\delta \alpha}{\delta \alpha_0} + w_t \frac{\delta t}{\delta t_0} \quad (1)$$

where δp, $\delta\alpha$ and δt are respectively the Euclidian distance, the shift angle and the duration between the current detection and the last detection of the considered track. Weights w_p, w_α and w_t in Eq. (1) as well as the normalization quantities δp_0, $\delta\alpha_0$, and δt_0 are set beforehand. The detection is assigned to the track for which C is minimum. When $\delta p \geq \delta p_0$, $\delta\alpha \geq \delta\alpha_0$ or $\delta t \geq \delta t_0$, the detection generates a new track. This step is called *track assignment*. Once the track assignment step is performed for each permutation P_q, a number of Q updated set of tracks are obtained. To determine the best set of tracks among the Q possible sets of tracks, we proceed as follows:

(i.) Only sets of tracks with the lowest number of tracks are considered;

(ii.) Among the remaining sets of tracks, we compute the averaged cost function $\widehat{C}$ over all tracks. Only sets for which $\widehat{C}<\widehat{C}_0$ are selected, where $\widehat{C}_0$ designates a threshold defined beforehand;

(iii.) Remaining sets of tracks are finally investigated by analyzing how detections correlate with the increasing timestamp. This investigation is carried out from the determination of the Spearman rank correlation coefficient. The set of tracks associated with the highest correlation coefficient is then selected.

The three steps defined above are part of the *tracks update* process. The complete tracks are obtained both for the forward and backward reconstruction methods when the *permutation*, the *track assignment*, and the *track update* steps are respectively applied to each gate D_m. To select which of the backward or forward tracks are kept, we select the solution with the smallest number of tracks. If the numbers of tracks are equal for both backward and forward reconstructions, then we compute the sum of the cost function C_{tot} over all gates. The reconstruction which minimizes the cost function is chosen. This last step of the MT² algorithm is called the *reconstruction method selection*.

The main factor impacting computation time of the MT² algorithm is the average number of detections within a gate. For a detection set D with M detections with uniformly-spaced timestamps, the number n_m of detections within each gate D_m is the same and therefore, the number of permutations of $Q=n_m!$ –and consequently, the computation time– can be reduced by shortening the time interval δt_s set beforehand. When the detection set D includes detections that are not uniformly-spaced in time, the number of detections per gate can be reduced to the maximum value n_{max}.

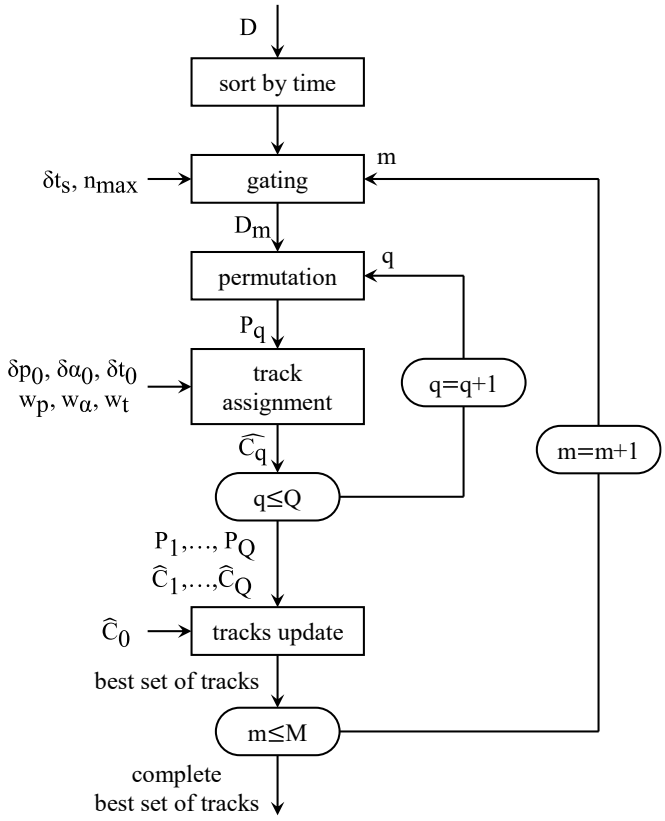

Fig. 2. Flowchart of the MT² algorithm from the detection set to the selected tracks (i.e., the complete best set of tracks) for a given (forward or backward) reconstruction method.

B. Performance evaluation of the MT² algorithm

To test the performance of the MT² algorithm, we simulate the tracks of two point targets (#1 and #2), one moving along the x-axis and the other along the y-axis (see Figure 1 for the definition of the axes). Each target is modeled by 10 detections. The

simulated trajectories of the targets cross at (x,y)=(0,0) with a small delay δt of 100ms at the angle β of 90°. Gaussian noise is added to the detection locations in x, y and z with the standard deviation σ of 5cm (Figure 3(a)). N_c=5 clutter detections (or false detections) are added, which locations are generated randomly. Next, we apply the MT² algorithm on the set of unclassified detections and obtain the tracks shown in Figure 3(b). The parameters of the algorithm were set beforehand with the following values: δp_0=0.5, $\delta\alpha_0$=180°, δt_0=300ms, w_p=1, w_α=1, w_t=1 and δt_s=150ms. Six tracks are obtained from both the forward and backward reconstructions, and the total cost for the forward reconstruction (C_{tot}=20.36) is found lower than the total cost obtained from the backward reconstruction (C_{tot}=20.58). Therefore, tracks provided by the forward reconstruction are selected here. To evaluate the comparison between the estimated tracks with ground-truth tracks, we use the standard *Association Accuracy* (AssA) metric detailed in [11]. We obtain a higher AssA score for the forward reconstruction (0.85) compared with the backward reconstruction (0.65). Therefore, the proposed MT² algorithm generates tracks using the forward reconstruction as its accuracy score is lower than that of the backward reconstruction.

We explore now the effect of the angle β between two trajectories at the crossing point (0,0) on the performance of the tracking algorithm by applying the Monte-Carlo approach. From Figure 4(a), we observe that the algorithm accuracy increases with angle β and therefore, the larger the angle between two tracks, the higher the accuracy of tracks reconstruction. The impact of the number of clutter detections N_c on the algorithm performance is also explored using the Monte-Carlo approach. From Figure 4(b), we observe that, as expected, the higher the number of false detections, the lower the accuracy of tracks reconstruction.

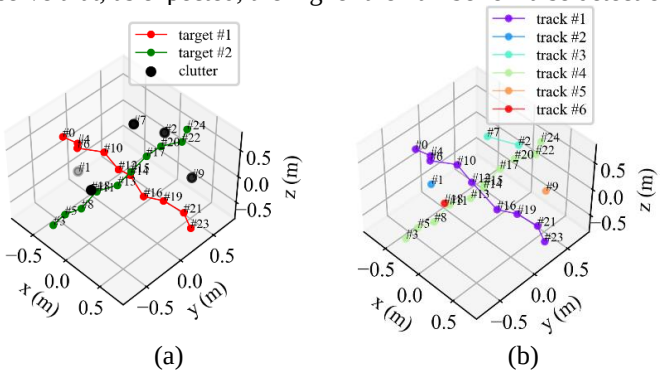

Fig. 3. Three dimensional representations of: (a) the ground-truth simulated targets tracks and clutter detections; (b) the tracks derived from the proposed MT² algorithm applied to the set of unclassified detections (using the forward reconstruction method). The detections are labelled by increasing timestamp.

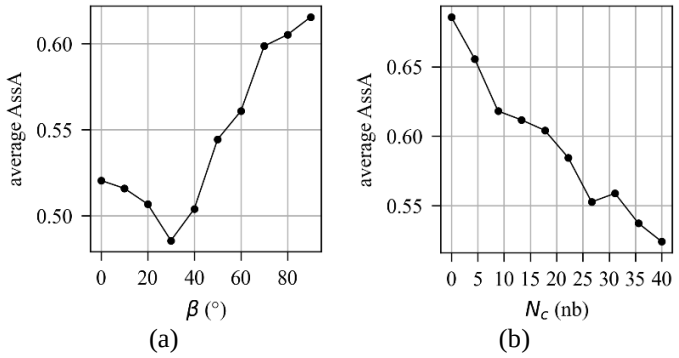

Fig. 4. Average accuracy (AssA) over 100 random experiments as a function of : (a) angle β between two trajectories at the crossing point (0,0); and (b) number N_c of clutter detections (i.e., of false detections).

IV. Application of the MT² Algorithm to Track Small Moving Targets

A. *Tracking of two tags moving in the scene*

To demonstrate experimentally the effectiveness of the MT² algorithm, we moved two metallic objects (2cm long metallic cylinders used to tag/equip bees [9]), one along the x-axis and the other along y-axis so as they cross at approximately 1.5m in front of the radar system. These measurements were carried out outside. To control their movement, tags were attached to a rod using a nylon thread. We first applied the detection algorithm of Section II.C to the radar images obtained from the collected raw data and next, we used MT² algorithm on the set of unclassified detections, as described in Section III. The parameters of the algorithm were set beforehand with values: δp_0=0.2, $\delta\alpha_0$=180°, δt_0=400ms, w_p=1, w_α=1, w_t=2, δt_s=60ms and n_{max}=4. The tracks provided by the MT² algorithm are then classified as clutter (75.3%) if they include less than 10 detections or if their total duration is shorter than 0.5s. Otherwise, the tracks are classified as target tracks (24.7%). The resulting tracks are displayed in Figure 5(a).

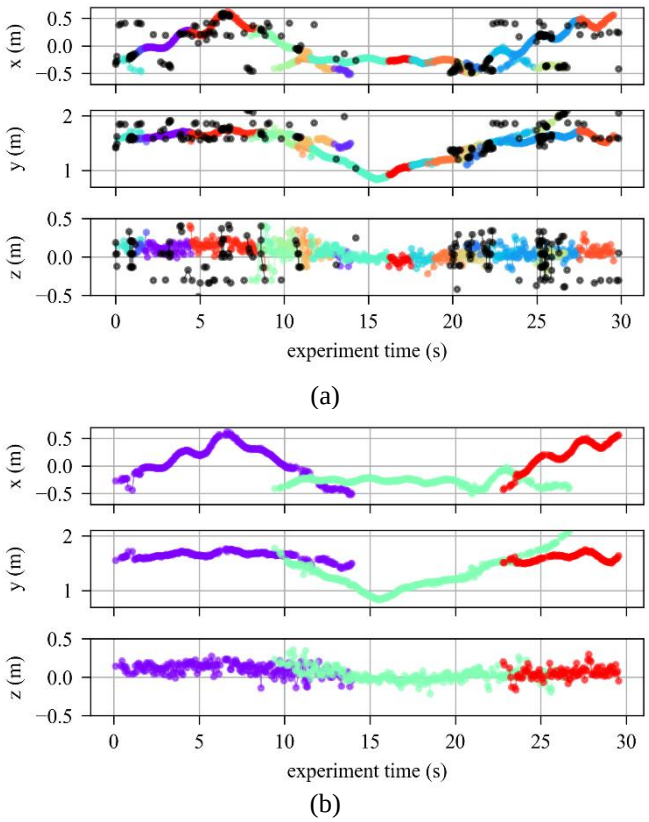

Fig. 5. Tracks of two moving tags obtained from the application of the MT^2 algorithm: (a) raw target tracks (the classification step allows discriminating clutter which is shown in black, while each target track is indicated in a unique colour); (b) corrected tracks obtained from applying the correction algorithm to the target tracks. Tracks #1, #2 and #3 are respectively in purple, green and red.

Finally, to join successive tracks that are likely to correspond to the same target, a set of *corrected* target tracks is generated using a similar assignment strategy as in Section III.A. Therefore, track-to-track associations are derived sequentially from the minimization of a cost function at each step. From application of this correction process to the set of target tracks, we derive the three tracks shown in Figure 5(b), that is, tracks #1 and #3 of tag #1 and track #2 of tag #2. Two separate tracks occurred for tag #1 because it was moved outside of the detection volume of the radar scanning system.

V. Conclusion

We introduced a so-called *Multi-Target Tracking* algorithm to track several small moving targets from a mm-wave FM-CW radar system. The algorithm is simple to implement compared with most multi-object tracking algorithms currently used, and it does not require prior knowledge of the number of targets to tracks (as, e.g., in Probabilistic Data Association Multi-Target Tracking Filters [12]). The next step is to use the algorithm for tracking tagged bees flying between their nest and a feeder.

Acknowledgment

We thank the ANR (French Research Agency) for financial support through the 3DNaviBee project (ANR-19-CE37-0024).

References

[1] M. Lihoreau and A. Duncan, *What Do Bees Think About?* Johns Hopkins University Press, 2024. doi: 10.56021/9781421448589.

[2] I. Ahmed and I. A. Faruque, 'High speed visual insect swarm tracker (Hi-VISTA) used to identify the effects of confinement on individual insect flight,' *Bioinspir. Biomim.*, vol. 17, no. 4, p. 046012, Jun. 2022. doi: 10.1088/1748-3190/ac6849.

[3] C.-H. Chen, A.-S. Chiang, and H.-Y. Tsai, 'Three-Dimensional Tracking of Multiple Small Insects by a Single Camera,' *J. Insect Sci.*, vol. 21, no. 6, p. 14, Nov. 2021. doi: 10.1093/jisesa/ieab079.

[4] J. D. Crall, N. Gravish, A. M. Mountcastle, and S. A. Combes, 'BEEtag: A Low-Cost, Image-Based Tracking System for the Study of Animal Behavior and Locomotion,' *PLOS ONE*, vol. 10, no. 9, p. e0136487, Sep. 2015. doi: 10.1371/journal.pone.0136487.

[5] E. Dedic, D. Henry, M. Lihoreau, and H. Aubert, '3D Motion Tracking of Flying Insects from a Millimeter-Wave Radar Imaging System,' *Computers and Electronics in Agriculture*. SSRN Preprint, Feb. 13, 2024. doi: 10.2139/ssrn.4725154.

[6] L. Rakai, H. Song, S. Sun, W. Zhang, and Y. Yang, 'Data association in multiple object tracking: A survey of recent techniques,' *Expert Syst. Appl.*, vol. 192, p. 116300, Apr. 2022. doi: 10.1016/j.eswa.2021.116300.

[7] J. Smith, F. Particke, M. Hiller, and J. Thielecke, 'Systematic Analysis of the PMBM, PHD, JPDA and GNN Multi-Target Tracking Filters,' *22th International Conference on Information Fusion*, Ottawa, ON, Canada, July 2-5, 2019, pp. 1–8. doi: 10.23919/FUSION43075.2019.9011349.

[8] G. O. Manokhin, Z. T. Erdyneev, A. A. Geltser, and E. A. Monastyrev, 'MUSIC-based algorithm for range-azimuth FMCW radar data processing without estimating number of targets,' *15th Mediterranean Microwave Symposium*, Lecce, Italy, November 30 - December 2, 2015, pp. 1–4. doi: 10.1109/MMS.2015.7375471.

[9] E. Dedic, A. Hadj Djilani, D. Henry, M. Lihoreau, and H. Aubert, '3D Tracking of Small Moving Targets in Cluttered Environment from the Isolines Processing of Millimeter-wave Radar Images,' *International Symposium on Antennas and Propagation and USNC-URSI Radio Science Meeting*, Portland, Oregon, USA, July 23-28, 2023, pp. 1233-1234. doi: 10.1109/USNC-URSI52151.2023.10237829.

[10] D. Henry and H. Aubert, 'Isolines in 3D Radar Images for Remote Sensing Applications,' *16th European Radar Conference* (EuRAD), Paris, France, October 2-4, 2019, pp. 69-72.

[11] J. Luiten *et al.*, 'HOTA: A Higher Order Metric for Evaluating Multi-object Tracking', *Int. J. Comput. Vis.*, vol. 129, no. 2, Feb. 2021, pp. 548–578. doi: 10.1007/s11263-020-01375-2.

[12] Y. Bar-Shalom, F. Daum, and J. Huang, 'The probabilistic data association filter', IEEE *Control Syst. Magazine*, vol. 29, n° 6, Dec. 2009, pp. 82–100. doi: 10.1109/MCS.2009.934469.